Mechanism and Reactivity of Alkane C−H Bond Dissociation on Coordinatively Unsaturated Aluminum Ions, Determined by Theoretical Calculations

Dan Fărcaşiu* and Povilas Lukinskas

Department of Chemical and Petroleum Engineering, University of Pittsburgh, 1249 Benedum Hall, Pittsburgh, Pennsylvania 15261

Received: October 8, 2001

DFT calculations at the B3LYP/6-31G** level were conducted on the reaction of the propane molecule with the aluminum hydroxide clusters $(HO)_3Al(OH_2)_x$ ($x = 0,1$). Weak, physisorbed (van der Waals) complexes were identified. Chemisorption does not involve the Brønsted acidity of the catalyst, as no hydron transfer occurs. Instead, the reaction involves insertion of the aluminum atom into a C−H bond, followed by the migration of the hydrogen atom from aluminum to oxygen, to form the chemisorbed intermediate, $(H_2O)_{x+1}(HO)_2Al-CH_2Et$ or $(H_2O)_{x+1}(HO)_2Al-CHMe_2$, with the latter having a higher energy barrier. The elimination of hydrogen from Cβ and oxygen gives then H_2 and propene, which forms a strong π complex with the aluminum cluster for $x = 0$. The first step, chemisorption, has a lower energy barrier than the second, elimination, but still higher than the hydrogen dissociation on the same clusters. Thus, the rate relationship H_2/D_2 exchange > H_2/RH exchange > RH dehydrogenation is predicted, as was experimentally observed. The tetracoordinated aluminum cluster ($x = 1$) reacts with the hydrocarbon by the same pathway as the tricoordinated aluminum cluster ($x = 0$) but with higher barriers for both steps; the barriers are reduced for the larger cluster $(HO)_2(H_2O)Al-O-Al(OH)_2(H_2O)$. The alternative pathway, forming the alkyl−oxygen adduct $(HO)_2Al(OH_2)_x(H)-O(R)H$ is too high in energy to compete. Examination of butane and isobutane establishes the reactivity order: prim C−H > *sec*-C−H > *tert*-C−H. For isobutane, essentially only methyl C−H cleavage should occur in the common first step for hydrogen exchange and dehydrogenation. In the second step, i.e., the β C−H cleavage in the Al-alkyl intermediate, the reactivity order is *tert*-C−H > *sec*-C−H > prim C−H. "Broken lattice" zeolites and especially extraframework aluminum species present in steamed zeolites should be more reactive than the intact zeolite lattices. Thus, the mechanism is relevant for the activation of alkanes for acid-catalyzed conversions on these catalysts, which have insufficient acid strength to cleave C−H and C−C bonds by hydron transfer.

Introduction

Active forms of aluminum oxide catalyze the exchange between elemental hydrogen and deuterium (through the exchange with the OH group of the catalyst)[1] and the H−D exchange of saturated hydrocarbons.[2] Both these reactions have been described as examples of acid−base catalysis.[2] More specifically, following the developments of concepts of superacid chemistry, the reactions of hydrocarbons on solid acids, particularly aluminosilicates, have been generally interpreted as involving the activation of reactant by hydron transfer to form carbocations, either as intermediates or as transition structures.[3]

The computational studies of the activation of C−H bonds in alkanes have usually attempted to describe the accepted mechanism and, therefore, sought mostly pathways based on hydron transfer.[4] Likewise, the dissociation of hydrogen on aluminum hydroxide clusters was assumed to involve a heterolytic cleavage of the hydrogen−hydrogen bond, with the hydron going to oxygen (basic site) and the hydride going to aluminum (acid site). MO calculations, both semiempirical[5] and ab initio without electron correlation,[6] following this postulated reaction pathway, were conducted.[5,6] We noted, however, deficiencies in those calculations and conducted a computational study of the dissociative chemisorption of hydrogen on coordinatively unsaturated aluminum centers. In it, standard ab initio and DFT calculations were conducted with large basis sets (6-31G* to 6-311++G**) and electron correlation (MP2 and B3LYP, respectively).[7] They showed that the chemisorption occurs through the interaction of H_2 with the aluminum until both hydrogen atoms are bonded to Al, after which one hydrogen migrates to an adjacent oxygen atom. Thus, the reaction is better described as metal ion catalysis, rather than acid−base catalysis.[7] It is thus similar to the chemisorption of hydrogen on noble metals, with the migration of one hydrogen to a different atom (oxygen), akin to the extensively discussed spillover process.[8]

Another notable result of our calculations was that tri-, tetra-, and pentacoordinated aluminum atoms were all active in hydrogen dissociation, with the reactivity decreasing in that order.[7] The earlier reports had considered only tri- and pentacoordinated aluminum as potentially reactive,[5,6] but at the level of theory and with the constraints imposed to the system in those studies, the pentacoordinated species did not chemisorb hydrogen.[6b] For some obscure reason, the tetracoordinated aluminum had been considered coordinatively saturated by the workers in the field. Considering the concentrations of sites on alumina surfaces (typically 30% tetracoordinated; much less, but sometimes observed, pentacoordinated; immeasurably low, if at all, tricoordinated),[9] we concluded that tetracoordinated

* To whom correspondence should be addressed. Phone: 412-624-7449. Fax: 412-624-9639. E-mail: dfarca@pitt.edu.

10.1021/jp013724l CCC: $22.00
Published on Web 02/05/2002

sites are most likely responsible for the catalytic activity of γ- and η-alumina.[7] A tetracoordinated aluminum atom connected to a silicon by an oxygen bridge was also found to chemisorb hydrogen by this mechanism, but with a higher potential energy barrier (PEB) than the corresponding two-aluminum cluster, thus showing that extraframework aluminum species should be more active than the intact zeolite structures.[7]

We also conducted a computational search in which the reaction pathway was not presupposed for the reaction of small alkanes with the same aluminum oxide clusters.[10] As in the previous study, we have considered both one-aluminum clusters, $(HO)_3Al(OH_2)_x$ (**1**, $x = 0$; **2**, $x = 1$) and the two-aluminum cluster $(HO)_2(H_2O)Al-O-Al(OH)_2(H_2O)$ (**3**). Like there, we did not attempt to extrapolate from the clusters to models of the solid, for instance by the application of periodic boundary conditions. Such an approach assumes that the entire unit cell, including the reactant, is periodically repeated,[11] which is not expected of catalytic alumina. Moreover, embedding the structural moiety into the surface should affect more the energies of reaction and activation than the mechanism of reaction and relative reactivity of sites of different structure, which were our goals. It was important to conduct our calculations at a satisfactory level of theory, with a large basis set. Also, it was reported that the errors from neglect of long-range electrostatic effects are less important than the errors from inadequate optimization of structures.[12] Furthermore, experimental activation energies of catalytic reactions conducted at high temperatures are not necessarily chemistry-derived. One runs the risk of trying to duplicate computationally activation energies of reactions that are transport-limited! A comparison of the results obtained for the double clusters with the results obtained for the one-aluminum clusters allows to establish the effect of the neighboring aluminum center on the chemisorption at the reactive aluminum center. The small clusters are, of course, appropriate for modeling the extraframework aluminum species present in steamed zeolites.[13]

Finally, we have examined the relative reactivity of primary, secondary, and tertiary C−H bonds, using as model reactants propane, butane, and isobutane. The results are reported in full, below.

Computational Method

Most calculations were conducted with the program Gaussian 98;[14] only the STQN calculations, for which Gaussian 98 did not perform well, were conducted with the Gaussian 94 program,[15] all in the same manner as in the study of hydrogen chemisorption.[7] Standard ab initio calculations[16] with electron correlation and sufficiently large basis sets were not possible for the large systems studied in this work. Therefore, all geometry optimizations were conducted with the DFT-B3LYP method[17] and the 6−31G** basis set, with some MP2(FC)/6-31G** geometry optimizations run for comparison. Frequency analyses, giving also the zero-point energy corrections (ZPE),[16c] were conducted at the same level of theory. Transition structure searching by the STQN (synchronous transit-guided quasi Newton) method[18] and reaction pathway identification by the intrinsic reaction coordinate (IRC)[19] tracking were conducted in the standard manner.

No corrections were made for the basis set superposition error (BSSE).[20] They would affect mostly the energies of the physisorbed complexes and would be, therefore, inconsequential.

The computer program Molden[21] was used for the assignment of calculated frequencies to specific vibrations. The projections of structures shown in the figures were generated with the program XMol.[22]

Results and Discussion

1. Reaction of Propane on the Tricoordinated Aluminum Cluster. The geometry of the aluminum hydroxide reactant **1** was chosen based on the consideration that transitional aluminas are formed by the calcination of a hydrated aluminum oxide, like boehmite. One can consider that the bulk of the solid is already set to a significant extent at the boehmite stage and the structural reorganization upon calcination affects mostly the surface.[23] We optimized, therefore, the geometry of the hydrated cluster **2** as the starting point and then removed the extra water molecule to obtain the corresponding reactive (coordinatively unsaturated) cluster **1** (eq 1).[7]

Two types of constraints were applied in our study of the reaction of hydrogen with **1**. In the first (A), the O1−O2−Al−O3 dihedral angle was kept constant at the same value as in **2** and the other geometrical parameters were optimized. In the alternative mode (B), the outer atoms of **1** were frozen in the position they had in the hydrated cluster **2** and the geometry of the central fragment (the Al $(-O-*)_3$ group) was optimized. The reaction proceeded in the same way in either mode and the PEB for the formation of the chemisorbed complex was the same for both.[7a] The reaction of **1** with the larger molecule, propane, was investigated only in mode A. Because there is no evidence that tricoordinated aluminum species exist at all in active alumina or zeolites, we concentrated on the reaction of the tetracoordinated aluminum cluster **2**, on which no geometry constraints were placed (see below). The reaction pathways calculated for clusters **1** and **2** were the same in every detail. Thus, even if the energy barriers for the reaction of **1** along pathways A and B were different, that finding would not affect the conclusions. Moreover, the reaction pathway for the reaction of the C−H bonds was in each case the same as that for the reaction of the H−H bond, where the same PEB was found for modes A and B.[7a]

$$\underset{\mathbf{2}}{(HO)_3Al-OH_2} \rightarrow \underset{\mathbf{1}}{(HO)_3Al} + H_2O \qquad (1)$$

The calculations have established the existence of a weak complex of **1** with propane (physisorbed propane), of the van der Waals type (**4**), 4 kcal/mol[24] more stable than the isolated reactants (without a BSSE correction). Two kinds of chemisorption products were identified, with alkyl-aluminum bond (**5**) and with alkyl-oxygen bond (**6**), illustrated for **1** by eqs 2 and 3, respectively, with $x = 0$. For each type of complex, the catalyst cluster can cleave either a primary or a secondary C−H bond (series **a** and **b** in eqs 2 and 3).

$$\underset{\mathbf{1}\ (x=0),\ \mathbf{2}\ (x=1)}{(HO)_3Al(OH_2)_x} + PrH \rightarrow \underset{\mathbf{5}\ (x=0),\ \mathbf{8}\ (x=1)}{(HO)_2Al(OH_2)_{x+1}(R)} \qquad (2)$$

$$\mathbf{1}, \mathbf{2} + PrH \rightarrow \underset{\mathbf{6}\ (x=0),\ \mathbf{9}\ (x=1)}{(HO)_2Al(OH_2)_x(H)\text{-}O(R)H} \qquad (3)$$

a: R = 1-Pr **b**: R = $CHMe_2$

The transition structure for the chemisorption step on the alkyl-aluminum pathway, identified by the STQN method,[18] was similar to the transition structure for hydrogen chemisorption. The imaginary frequency was identified as the bending of the Al−H bond toward O, that is, the migration of hydrogen from aluminum to oxygen.[21] The transition structure (TS1) for

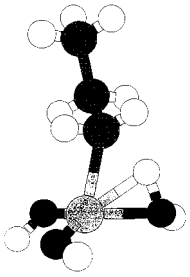

Figure 1. Transition structure (TS1) for the chemisorption of propane (methyl C−H cleavage) by C−Al bonding, on a tricoordinated aluminum cluster (**1** → **5a**).

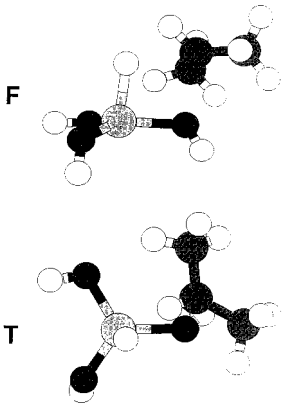

Figure 2. Transition structure (TS1) for the chemisorption of propane (methylene C−H cleavage) by C−O bonding, on a tricoordinated aluminum cluster (**1** → **6b**). F = front view, T = top view.

chemisorption on the tricoordinated cluster, **1** → **5a**, is shown in Figure 1.[22] IRC tracking verified the transition structures. In the transition structure, the distance of the migrating hydrogen to the oxygen is 20−25% longer than the normal O−H bond, whereas its distance to aluminum is only 10−15% longer than the normal Al−H bond. Most importantly, however, the Al−H distance is even shorter prior to the transition state and then increases, whereas the O−H distance decreases throughout the process. Thus, the reaction mechanism consists of the insertion of aluminum into the C−H bond, followed by hydrogen migration from Al to O, just like for hydrogen chemisorption.[7]

The alternative, alkyl−oxygen, pathway **1** → **6b** (eq 3), was closer to a concerted four-center process. Its transition structure, TS1, is shown in two projections in Figure 2. The C−O bond formation seemed to lag somewhat behind the Al−H bond formation. The charge distribution (Mulliken population analysis) showed that the reacting carbon acquired a positive charge on the pathway of eq 3 (**1** → **6b**); therefore, the corresponding reaction of a primary C−H bond (**1** → **6a**) should be of significantly higher energy and was not investigated.

The products of chemisorption on either pathway can react further, to form hydrogen and propene. It is well established that alkenes can be hydrogenated and alkanes dehydrogenated on alumina and on silica−alumina catalysts.[25] Locating a transition structure for the elimination from the O-alkyl complex **5** was a trivial matter, as the reaction proceeded smoothly over a cyclic transition structure (TS2, Figure 3),[22] in a process reminiscent of the thermal elimination of esters, leading to propene and the complex with chemisorbed hydrogen (adduct) on the aluminum cluster (eq 4). The hydrogen was transferred from Cβ to another oxygen atom. It was much more difficult, however, to map the reaction pathway for the elimination from the alkyl-aluminum complexes **5a** and **5b**. The STQN method was not successful, because we did not have the structure of

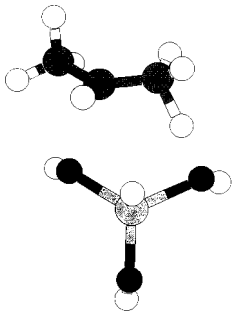

Figure 3. Transition structure (TS2) for the elimination of propene from the alkyl-oxygen adduct, **6b** (top view).

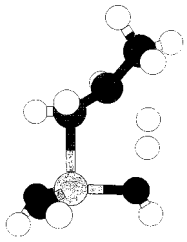

Figure 4. Transition structure (TS2) for the elimination of propene from the alkyl-aluminum adduct, **5a**.

the final state of the reaction. We were able to find the transition structure by standard Berny optimization of various candidates. The structure that we obtained was confirmed by IRC[19] tracking, which also gave the structure of the elimination product. The latter was a π complex of propene with the aluminum cluster (**7**), formed together with a hydrogen molecule, which is also physisorbed on the cluster, but only weakly (eq 5). The coordinatively unsaturated aluminum atom binds much stronger to a carbon−carbon double bond ($\Delta E = -11.9$ kcal/mol for the complexation of propene to give **7**) than to a molecule of hydrogen ($\Delta E = -1.78$ kcal/mol for the complexation of H_2 to **1**, at B3LYP/6-31G** without ZPE correction).[7a] The former is a π complex, and the latter is a van der Waals complex. There was much less cleavage of the Al−C bond than of the C−H bond at the transition state of the second step (TS2, shown in Figure 4, for the decomposition of **5a**).[22]

$$\mathbf{6b, 9b} \rightarrow \text{H-Al(OH)}_2(\text{-OH}_2)_{x+1} + \text{Me-CH=CH}_2 \quad (4)$$

$$\mathbf{5a, 5b, 8a} \rightarrow (\text{HO})_3(\text{H}_2\text{O})_x\text{Al-}\overset{\text{CH}_2}{\underset{\text{CHMe}}{\|}} + \text{H}_2 \quad (5)$$

$$\mathbf{7}\ (x = 0),\ \mathbf{10}\ (x = 1)$$

For comparison, we also examined the reaction coordinate for the alkyl-aluminum chemisorption pathway **1** → **5a** by MP2/6-31G** geometry optimization. The structures obtained were essentially the same, confirming the conclusion of the study of hydrogen chemisorption, in which the equivalency of the MP2 and B3LYP calculations was thoroughly tested.[7]

The energies of intermediates and products, relative to the starting materials, are shown in Table 1. As seen in the table, the alkyl−aluminum complexes were found more stable than the alkyl-oxygen complex **6b** by 6.1 kcal/mol (**5a**) and 3.8 kcal/mol (**5b**). The reaction coordinates for the two pathways were quite different. Thus, the chemisorbed complexes of eq 2 (Al−C bonding) represented shallow energy minima with low barriers (1−2 kcal/mol) for the return to reactants. The rate-determining step for the dehydrogenation was the elimination from **5**. About half of the energy barrier for dehydrogenation came from the endothermicity of the reaction (29.2 kcal/mol for the conversion

TABLE 1: Calculated Relative Energies of Intermediates, Products, and Transition Structures for the Reaction of Propane with the Aluminum Hydroxide Clusters 1, 2, and 11[a]

reaction pathway	physisorbed reactant [b]	TS1	chemisorbed complex	TS2	physisorbed product(s)[b]	isolated products
			A. Tricoordinated Aluminum Cluster (**1**) as Catalyst			
Al−CH_2Et[c]	−4.01	32.19	31.24	57.10	17.63	29.23
Al−CH(Me)$_2$[d]	−4.01	35.14	33.54	62.41	17.63	29.23
Al−CH(Me)$_2$[e]	−6.33	33.59	31.50			
O−CH(Me)$_2$[f]	−4.01	72.31	37.34	70.35	46.65[g]	29.23[h]
			B. Tetracoordinated Aluminum Cluster (**2**) as Catalyst			
Al−CH_2Et [i]	−1.93	43.95	25.59	74.20 [j] 72.21[k]	26.56	29.23
Al−CH(Me)$_2$[l]	−1.93	*m*				
O−CH(Me)$_2$[n]	−1.93	82.22	32.28	75.98[o] 67.31[p]	43.77	29.23[q]
			C. Two-Aluminum (Both Tetracoordinated) Cluster (**11**) as Catalyst			
Al−CH_2Et[r]	−3.77	37.02	20.89[s]	67.01[t]	20.49	29.23

[a] B3LYP/6-31G**//B3LYP/6-31G** + ZPE, kcal/mol, relative to the isolated starting materials (**1**, **2**, or **11** and PrH). [b] The values in this column are affected by basis set superposition errors. [c] **1** → **5a**, eq 2, then eq 5. [d] **1** → **5b**, eq 2, then eq 5. [e] MP2(FC)/6-31G**//MP2(FC)/6-31G** values. [f] **1** → **6b**, eq 3, then eq 4. [g] Propene physisorbed on the $(HO)_2AlH-OH_2$ cluster. [h] 44.98 kcal/mol if $(HO)_2AlH-OH_2$ is a product. As the energy for the latter was not ZPE-corrected, the number is only orientative. [i] **2** → **8a**, eq 2, then eq 5. [j] d(Al−OH_2) = 2.11 Å, as in the chemisorbed complex, **8a** (see text). [k] d(Al−OH_2) = 2.31 Å, see text. [l] **2** → **8b**, eq 2. [m] Decomposition to **5b** occurred. [n] **2** → **9b**, eq 3, then eq 4. [o] d(Al−OH_2) = 2.00 Å, as in the chemisorbed complex, **9b** (see text). [p] d(Al−OH_2) = 2.20 Å, see text. [q] 48.14 kcal/mol, if $(H_2O)_2AlH(-OH)_2$ is a product.[r] eq 6. [s] Adduct **12**. [t] d(Al−OH_2) = 2.136 Å, as in the chemisorbed complex, **12** (see text).

SCHEME 1: Reaction Coordinate for Propane Dehydrogenation (Aluminum−Alkyl Pathway, Eqs 1 and 5, $x = 0$, Path a)

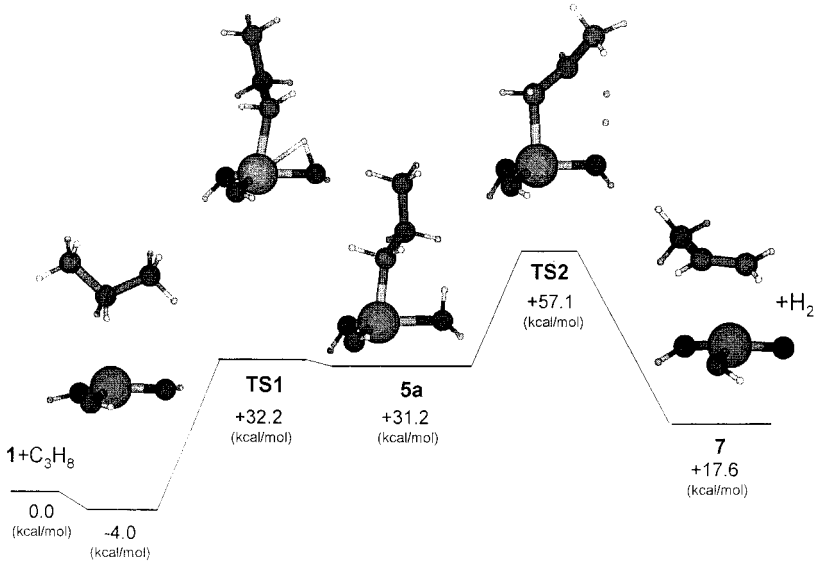

of propane to propene at B3LYP/6-31G** with ZPE correction). Both the chemisorbed intermediate and the two transition structures were lower in energy for the reaction of the primary C−H (**a**). This result can be rationalized by electronic factors, because the negative electric charge at the reacting carbon increased during the chemisorption (it was highest in the transition structure), but a contribution from steric factors needs also to be considered.

Contrastingly, the mechanism of eq 3 (O-alkyl pathway) has high energy barriers on both sides of the chemisorbed intermediate, with the barrier for the first step being slightly higher (by 2 kcal/mol). It can be safely concluded that both hydrogen exchange and dehydrogenation/hydrogenation occur exclusively by the alkyl−aluminum pathway. The potential energy profile of the lowest energy pathway (over **5a**) for propane dehydrogenation/propene hydrogenation on the aluminum cluster **1** is presented in Scheme 1. The energy shown for the product, **7**, includes the stabilizing interaction with the hydrogen molecule (−0.6 kcal/mol, again without BSSE correction).

A comparison between an alkyl-metal and an alkyl-oxygen pathway was recently reported for the dehydrogenation of ethane by the gallium atom of a cluster in which a H_2Ga moiety was bonded to two tricoordinated (oxonium) oxygens of an aluminosilicate model.[26] The gallium-bonded hydrogens were involved in the reaction (a Ga−H bond was broken upon ethane chemisorption and a Ga−H bond was formed in the elimination step). The alkyl-metal pathway was also found the lower-energy process in that system.[26]

2. Reaction of Propane on Tetracoordinated One-Aluminum and Two-Aluminum Clusters. Because a tetracoordinated aluminum atom inherently has less flexibility than a tricoordinated atom, the geometry optimizations were conducted without any restraints. No chemisorbed complex of formula **8b** (eq 2) was identified in this way, however, because a water molecule dissociated and the reaction product was **5b**, described above. If the catalytic center was part of a solid, the lattice rigidity would prevent Al−O dissociation; therefore, chemisorption accompanied by a relaxation of the lattice

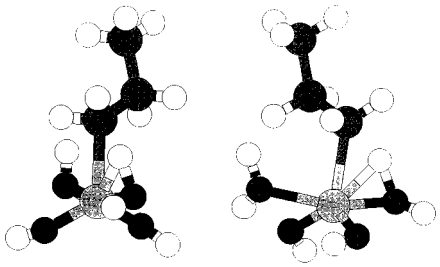

Figure 5. Transition structure (TS1) for the chemisorption of propane (methyl C−H cleavage) by C−Al bonding, on a tetracoordinated aluminum cluster (**2** → **8a**). F = front view, S = side view.

(increase of the O−Al bond length) should occur. As both the chemisorbed intermediate and the barrier for its formation were shown in the reaction with cluster **1**, above, to be higher in energy for the secondary C−H bond than for the primary C−H bond, the formation and reaction of **8b** were not investigated further.

The reaction of the tetracoordinated aluminum cluster **2** was mechanistically the same as the reaction of the tricoordinated cluster, **1**, both for the alkyl-aluminum pathway (**2** → **8a**, eq 2) and for the alkyl-oxygen pathway (**2** → **9b**, eq 3). The transition structure for chemisorption (TS1) of propane on **2** by eq 2 is shown in Figure 5. In the second step of the reaction, both **8a** and **9b** eliminated easier water than propene. Depending upon the rigidity of the lattice around the aluminum center, three possibilities have to be considered. (1) If the system was fully flexible, the elimination would occur as for the tricoordinated aluminum cluster **1**, with the energy barriers calculated above, after which the broken aluminum−oxygen bond would be reformed. (2) If the lattice was rigid, the Al−O bond length would be preserved throughout elimination from both **8a** and **9b**; the calculation with this assumption provides the highest limit for the decomposition energy barrier. (3) For a lattice endowed with some local flexibility (the most likely case), the Al−O would be lengthened to some extent at the transition state for elimination; the energy barrier would be lower than in case 2 but not necessarily higher than in case 1, because secondary interactions assisting the elimination might exist. Optimization of the transition structures for the elimination steps from **8a** and **9b** were conducted for Al−OH_2 distances frozen as in the chemisorbed complexes (case 2) and longer by 0.2 Å (case 3).

The calculated energies are shown in the second section of Table 1. It can be seen that the calculated PEB for the rate-determining steps of both the alkyl−aluminum pathway (elimination step) and the oxygen−aluminum pathway (the propane chemisorption step) were higher than in the reaction catalyzed by the tricoordinated aluminum cluster, **1**. The same relationship between tri- and tetracoordinated aluminum clusters was found for hydrogen chemisorption.[7] The complexation of propene by the tetracoordinated cluster is weak (ca 3 kcal/mol). Therefore, structure **10** in eq 5 should be considered as a van der Waals complex.

The chemisorption and elimination by the alkyl−aluminum pathway were also examined for the double (tetracoordinated-tetracoordinated) cluster, **11**. The geometry of this catalyst was generated in our previous work by the optimization of the hydrated species, $(H_2O)_2Al(OH)_2-O-Al(OH)_2(H_2O)$, and removal of a molecule of water.[7b] The oxygens in the terminal hydroxy groups (drawn in bold letters in eq 6) were frozen, and the geometry of the dehydrated cluster was optimized with these constraints, modeling the anchoring of the active site onto the lattice.[7b] The same constraints were kept in the optimization of the species resulting from the interaction of **11** with propane (eq 6).

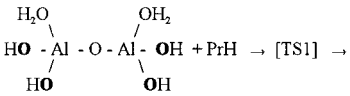

11

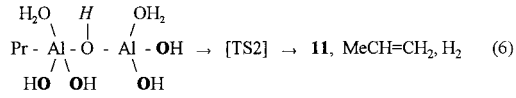

12

In the complex with chemisorbed propane, the hydrogen cleaved from a carbon went to the bridging oxygen, as expected.[7b] Otherwise, the reaction mechanism was the same as for the one-aluminum cluster **2**, and the Al−O bond also cleaved easier than the Al−C bond in the decomposition of the adduct **12**. Therefore, the transition structure for the elimination step (TS2) was optimized with the Al−OH_2 bond length frozen as in **12** (2.136 Å), to obtain the high limiting value of the potential energy barrier for elimination (option 2, above). The elimination is the rate-determining step of propane dehydrogenation on the dialuminum oxide-hydroxide cluster as well. Again as expected,[7b] all of the species along the reaction coordinate (intermediates and transition structures) are lower in energy for the two-aluminum cluster than for the one-aluminum cluster as catalyst (third section of Table 1).

On the basis of the close similarity observed in every point between the previous results on hydrogen dissociation[7] results and the present data on propane dehydrogenation, we can expect that a silicon−aluminum oxide model (hydrated) should also catalyze the latter reaction, but the energy barriers for the reactions should be higher than for the all-aluminum clusters.[7b] This prediction agrees with the comparative study by Holm and Blue of ethylene hydrogenation at 500 °C on alumina and silica−alumina catalysts.[25a]

3. Reaction of Butanes on the Tricoordinated Aluminum Cluster. The results shown above indicated that primary C−H bonds are more reactive than secondary C−H bonds toward the coordinatively unsaturated aluminum centers. To obtain further data on the relative reactivity of C−H bonds, we studied the reaction of butane (BuH) and isobutane (*i*-BuH) with cluster **1** on the alkyl−aluminum pathway (corresponding to Equations 2 and 5 for propane). The results are given in Table 2.

It is seen that the predicted relative reactivity of primary and secondary C−H bonds is the same for BuH as for propane. Moreover, the size of the hydrocarbon has little effect. Chain branching seems to have little effect on the alkane chemisorption (ca 1 kcal/mol difference between methyl C−H reactivity in BuH and *i*-BuH), but the elimination from the primary R−Al species has a lower barrier for the branched hydrocarbon than for the linear isomer.

A tertiary C−H bond of *i*-BuH is predicted to be less reactive than a secondary C−H bond of BuH by 3 kcal/mol for the dissociative chemisorption and by 5 kcal/mol for the elimination. An internal comparison of hydrogen atoms in *i*-BuH reveals a preference for the reaction involving initial insertion into a primary C−H bond over insertion into the tertiary C−H bond by 5.5 kcal/mol for dissociative chemisorption and by 13 kcal/mol for elimination.

4. Implications for Catalysis Mechanism. The calculations show that the hydrogen exchange with the catalyst has a much

TABLE 2: Calculated Relative Energies of Intermediates, Products, and Transition Structures for the Reaction of Butane and Isobutane with the Aluminum Hydroxide Cluster 1[a]

reacting bond	physisorbed reactant[b]	TS1	chemisorbed complex	TS2	physisorbed product(s)[b]	isolated products
$PrCH_2-H$[c]	−3.33	32.07	31.09	57.39	17.71	31.40
EtMeCH−H[c]	−3.33	35.88	34.65	62.45	17.71	31.40
EtMeCH−H [d]	−3.33	35.88	34.65	60.26	14.09[e]	25.68[e,f]
$(Me)_2CHCH_2-H$[g]	−4.14	33.26	31.63	54.25	12.76	30.62
Me_3C-H [g]	−4.14	38.82	35.09	67.31	12.76	30.62

[a] B3LYP/6-31G**//B3LYP/6-31G** + ZPE, kcal/mol, relative to the isolated starting materials (**1** and BuH or *i*-BuH). [b] The values in this column are affected by BSSE. [c] Reaction forming 1-butene. [d] Reaction forming 2-butene. [e] The value given is for *trans*-2-butene. [f] The value calculated for *cis*-2-butene is 28.52. [g] Reaction forming isobutene.

lower potential energy barrier than the elimination, for all clusters and for all types of C−H bonds. Therefore, it should be much faster than the elimination. We note that in the reaction of BuH-d_{10} with HZSM-5 at 400−550 °C, H−D exchange was at least 1 order of magnitude faster than dehydrogenation and cracking.[27] The chemisorption of hydrogen on the same clusters was found to have a smaller potential energy barrier[7] than the chemisorption of the alkane, which is in perfect agreement with the experimental results.[28] Therefore, the H_2/catalyst exchange should be the fastest process. Indeed, this rate relationship was found in a study of the reaction of tritium gas with toluene and with hexane on three zeolites.[29]

The difference in reactivity, prim C−H ≫ *tert*-C−H (with *sec*-C−H between) is clearly apparent for *i*-BuH, where it is compounded by a statistical factor of 9. Experimentally, no *tert*-C−H exchange was observed in isobutane at temperatures at which the methyl hydrogens exchanged readily.[4d,30] In the comparison of the primary C−H bonds in BuH and *i*-BuH, we must note that in the interaction with coordinatively unsaturated aluminum sites on an irregular surface, steric effects may determine the relative reactivity.

Mechanistically, our calculations show that the hydrogen exchange[2,4,27,30] and elimination reactions[25] of an alkane on materials containing $Al(O-)_n$ sites, with $n = 3$ and 4, are examples of metal ion catalysis.[7] The cleavage of H−H and C−H bonds by insertion of metal atoms and ions (metal and metal ion catalysis) has been well-known for heavy metals, particularly noble metals, but it was not considered for aluminum. An increase in reactivity for "broken lattices" of zeolites and a role for extraframework aluminum species of steamed zeolites in hydrogen and alkane activation is predicted by this mechanism.

Alkane activation by solid acids, particularly zeolites, was described as involving hydron transfer to C−H[3a] and C−C bonds,[3b] the same as for the liquid superacids HCl−$AlCl_3$ (or, rather, $H_2O-AlCl_3$),[31] HF−SbF_5,[32] and HF−TaF_5.[33] It was, indeed, claimed that zeolites, among others, are solid superacids.[34] Computational descriptions based on this reactivity model have been published.[4,35] The superacidity of solids has, however, been contested.[36] It was shown that solids are intrinsically much weaker acids than liquids of similar structure.[36b] In particular, the zeolite HZSM-5, for which the mechanisms involving hydronated alkanes with pentacoordinated carbon (carbonium ions) and cleavage of sigma bonds by acidolysis were put forward,[3] was shown to be much weaker than trifluoromethanesulfonic acid.[37] The latter is a weak superacid, capable of isomerizing and cracking alkanes, but the initiation appears to be by oxidation.[38] Activation of alkanes by zeolites through hydron transfer is, therefore, highly questionable.

Alternatively, a hydride abstraction by a surface Lewis acid site has been proposed for alkane activation.[30a] It was noted, however, that hydride abstraction from alkanes does not occur even with the much stronger Lewis acid, SbF_5.[39]

A reverse heterolysis of C−H bonds by aluminum oxide catalysts was also proposed. Thus, the reaction of methane with aluminum hydroxide was described as a heterolytic reaction with an acid−base pair on the surface, with the hydron going to the negative oxygen and a methyl anion to the metal.[40] It was computationally modeled by a process involving a concerted four-center reaction.[41] Formation of alkyl anions requires extremely high basicities, which cannot be expected of either the bridging oxygens or the hydroxylic oxygens present in active alumina. The insertion of the metal ion into the C−H bonds, predicted by the calculations, liberates the mechanistic model from such improbable acid−base reactions. It is noteworthy that the transition structure calculated (HF/6-31G) for the methane chemisorption along the postulated reverse C−H heterolysis pathway is somewhat similar to the one that we find for propane, but the critical feature that the hydrogen of the C−H bond to be broken has a bonding interaction with aluminum before migrating to oxygen was not evidenced in that study.[41]

Initiation of alkane reactions on solid acids by a one-electron oxidation has also been proposed.[42] Dehydrogenation on tricoordinated and especially tetracoordinated aluminum centers by the mechanism uncovered here represents an alternative alkane activation mechanism. An easier dehydrogenation on all-aluminum rather than on aluminum−silicon hydroxide clusters explains the effect of extraframework aluminum species in steamed zeolites on catalytic activity. It follows that for mechanistic studies on zeolites, the rigorous and sensitive identification and quantification of extraframework aluminum species is essential. Unfortunately, no good analytical procedure exists. The existence of extraframework aluminum species is normally concluded from the observation of hexacoordinated aluminum in the sample. The hexacoordinated aluminum is *inactive*, however. Moreover, for the cluster sizes possible inside the cavities, hexacoordination can be achieved only with molecules of water as ligands. The latter would be lost on calcination. Then, *the hexacoordinated aluminum species observed in steamed zeolites after thermal activation must be present on the external surface of crystals*. The active aluminum is tetracoordinated, present most likely as assemblies of two (or more) adjacent tetracoordinated aluminum atoms,[43] in agreement with our findings here. Therefore, it is hardly distinguishable by ^{27}Al NMR from the lattice aluminum.

The one-electron transfer and aluminum insertion might occur competitively. In either case, the critical intermediate is a bonded or complexed olefin. In the reactions on aluminosilicates, the barrier for reaction of the olefin with the acid site is lower than the barrier for hydrogenation; therefore, a cationic-type (cationoidic) reaction ensues. At high temperatures and low pressure, olefin products desorb from the catalyst. In experiments with the feed as liquid and at lower temperatures (120−160 °C),

however, only saturated hydrocarbons were desorbed from the catalyst, as isomerization and disproportionation products, but they were formed entirely via olefinic intermediates.[44] The isomerization of hexane under the same conditions on acid mordenite also cannot be rationalized by the clasical mechanism of sigma bond acidolysis and carbocationic rearangement.[45] All of these findings are consonant with the present calculations.

Acknowledgment. Support of our research of strong acid catalysis by the Grant CTS-9812704, from NSF, is gratefully acknowledged. A grant of supercomputer time was obtained from the National Center for Supercomputing Applications (NCSA) in Urbana, IL.

References and Notes

(1) (a) Taylor, H. S.; Diamond, H. *J. Am. Chem. Soc*. **1935**, *57*, 1256. (b) Lee, J. K.; Weller, S. W. *Anal. Chem*. **1958**, *30*, 1057. (c) Hall, W. K.; Leftin, H. P.; Cheselske, F. J.; O'Reilly, D. E. *J. Catal*. **1963**, *2*, 506. (d) Hall, W. K.; Lutinski, F. E. *J. Catal*. **1963**, *2*, 518. (e) Carter, J.; Lucchesi, P.; Corneil, P.; Yates, D. J. C.; Sinfelt, J. H. *J. Phys. Chem*. **1965**, *69*, 3070. (f) Garrett, B. R. T.; Rooney, J. J. *J. Chem. Soc., Perkin Trans. 2* **1974**, 960.

(2) For references, see: Yoshida, S. In *Theoretical Aspects of Heterogeneous Catalysis*; Moffat, J. B., Ed.; Van Nostrand Reinhold: New York, 1990; p 506.

(3) (a) Haag, W. O.; Dessau, R. M. *Proc. 8th Intl. Congr. Catal., Berlin 1984*, vol. 2; Dechema: Frankfurt-am Main, 1984; p 305. (b) Abbot, J.; Wojchechowski, B. *Ind. Eng. Chem. Prod. Res. Dev*. **1985**, *24*, 501. (c) Giannetto, G.; Sansare, S.; Guisnet, M. *J. Chem. Soc., Chem. Commun*. **1986**, 1302 (d) Hall, W. K.; Lombardo, E. A.; Engelhardt, J. *J. Catal*. **1989**, *115*, 611. (e) See the discussion in Fărcaşiu, D.; Lukinskas, P. *Rev. Roumaine Chim*. **1999**, *44*, 1091.

(4) (a) van Santen, R. A.; Kramer, G. J. *Chem. Rev*. **1995**, *95*, 637. (b) Kazansky, V. B.; Frash, M. V.; van Santen, R. A. *Appl. Catal., A* **1996**, *146*, 225. (c) Rigby, A. M.; Kramer, G. J.; van Santen, R. A. *J. Catal*. **1997**, *170*, 1. (d) Bates, S. P.; van Santen, R. A. *Adv. Catal.* **1998**, *42*, 1. (e) Zygmunt, S. A.; Curtiss, L. A.; Iton, L. E. *Abstracts, 16th Meeting of the North American Catalysis Society, Boston, MA, June 2*, **1999**, *119*. (f) Esteves, P. M.; Nascimento, N. A. C.; Mota, C. J. A. *J. Phys. Chem. B* **1999**, *103*, 10417.

(5) Zelenovskii, V. M.; Zhidomirov, G. M.; Kazanskii, V. B. *Zh. Fiz. Khim*. **1984**, *58*, 1788.

(6) (a) Senchenya, I. N.; Kazanskii, V. B. *Kinet. I Katal*. **1988**, *29*, 1331. (b) Ioka, F.; Sakka, T.; Ogata, Y.; Iwasaki, M. *Can. J. Chem*. **1993**, *71*, 663.

(7) (a) Fărcaşiu, D.; Lukinskas, P. *J. Phys. Chem. A* **1999**, *103*, 8483. (b) Lukinskas, P.; Fărcaşiu, D. *Appl. Catal. A* **2001**, *209*, 193.

(8) (a) Khoobiar, S. *J. Phys. Chem*. **1964**, *68*, 411. (b) Robell, A. J.; Ballou, E. V.; Boudart, M. *J. Phys. Chem*. **1964**, *68*, 2748. (c) Vannice, M. A.; Neikan, W. C. *J. Catal*. **1971**, *20*, 260. (d) Levy, R. V.; Boudart, M. *J. Catal*. **1974**, *32*, 304. (e) Fleisch, T.; Aberman, R. *J. Catal*. **1977**, *50*, 268. (f) Conner, W. C., Jr.; Pajonk, G. M.; Teichner, S. J. *Adv. Catal*. **1986**, *34*, 1. (g) Musso, J. C.; Parera, J. M. *Appl. Catal*. **1987**, *30*, 81.

(9) (a) Coster, D.; Blumenfeld, A. L.; Fripiat, J. J. *J. Phys. Chem*. **1994**, *98*, 6201. (b) Lee, M.-H.; Cheng, C.-F.; Heine, V.; Klinowski, J. *Chem. Phys. Lett*. **1997**, *265*, 673.

(10) Preliminary communication: Fărcaşiu, D.; Lukinskas, P. *Chem. Commun*. **2001**, 77.

(11) Schwarz, K.; Nusterer, E.; Blöchl, P. E. *Catal. Today* **1999**, *50*, 501.

(12) Sauer, J.; Ugliengo, P.; Garrone, G.; Saunders, V. R. *Chem. Rev*. **1994**, *94*, 2095.

(13) Shertukde, P. V.; Hall, W. K.; Marcelin, G. *Catal. Today* **1992**, *94*, 491.

(14) Frisch, M. J.; Trucks, G. W.; Schlegel, H. B.; Scuseria, G. E.; Robb, M. A.; Cheeseman, J. R.; Zakrzewski, V. G.; Montgomery, J. A., Jr.; Stratmann, R. E.; Burant, J. C.; Dapprich, S.; Millam, J. M.; Daniels, A. D.; Kudin, K. N.; Strain, M. C.; Farkas, O.; Tomasi, J.; Barone, V.; Cossi, M.; Cammi, R.; Mennucci, B.; Pomelli, C.; Adamo, C.; Clifford, S.; Ochterski, J.; Petersson, G. A.; Ayala, P. Y.; Cui, Q.; Morokuma, K.; Malick, D. K.; Rabuck, A. D.; Raghavachari, K.; Foresman, J. B.; Cioslowski, J.; Ortiz, J. V.; Stefanov, B. B.; Liu, G.; Liashenko, A.; Piskorz, P.; Komaromi, I.; Gomperts, R.; Martin, R. L.; Fox, D. J.; Keith, T.; Al-Laham, M. A.; Peng, C. Y.; Nanayakkara, A.; Gonzalez, C.; Challacombe, M.; Gill, P. M. W.; Johnson, B. G.; Chen, W.; Wong, M. W.; Andres, J. L.; Head-Gordon, M.; Replogle, E. S.; Pople, J. A. *Gaussian 98*, revision A.9; Gaussian, Inc.: Pittsburgh, PA, 1999.

(15) Frisch, M. J.; Trucks, G. W.; Schlegel, H. B.; Gill, P. M. W.; Johnson, B. G.; Robb, M. A.; Cheeseman, J. R.; Keith, T.; Petersson, G. A.; Montgomery, J. A.; Raghavachari, K.; Al-Laham, M. A.; Zakrzewski, V. G.; Ortiz, J. V.; Foresman, J. B.; Cioslowski, J.; Stefanov, B. B.; Nanayakkara, A.; Challacombe, M.; Peng, C. Y.; Ayala, P. Y.; Chen, W.; Wong, M. W.; Andres, J. L.; Replogle, E. S.; Gomperts, R.; Martin, R. L.; Fox, D. J.; Binkley, J. S.; Defrees, D. J.; Baker, J.; Stewart, J. P.; Head-Gordon, M.; Gonzalez, C.; Pople, J. A. *Gaussian 94*, revision D.3; Gaussian, Inc.: Pittsburgh, PA, 1995.

(16) (a) Pople, J. A. *Acc. Chem. Res*. **1970**, *3*, 217. (b) Pople, J. A. *Int. J. Mass Spectrom. Ion Phys.* **1976**, *19*, 89. (c) Hehre, W. J.; Radom, L.; Schleyer, P. v. R.; Pople, J. A. *Ab initio Molecular Orbital Theory*; Wiley-Interscience: New York, 1986.

(17) (a) Hohenberg, P.; Kohn, W. *Phys. Rev*. **1964**, *136*, B864. (b) Kohn, W.; Sham, L. *Phys. Rev.* **1965**, *140*, A1133. (c) Parr, R. G.; Yang, W. *Density Functional Theory of Atoms and Molecules*; Oxford University Press: New York, 1989. (d) Becke, A. D. *J. Chem. Phys.* **1993**, *98*, 5648.

(18) Peng, C.; Schlegel, H. B. *Isr. J. Chem*. **1993**, *33*, 449.

(19) Gonzales, C.; Schlegel, H. B. *J. Phys. Chem*. **1989**, *90*, 2154.

(20) Chalasiński, G.; Gutowski, M. *Chem. Rev*. **1988**, *88*, 943.

(21) Schaftenaar, G. *MOLDEN. A Portable Electron Density Program* Available at: ftp ftp.caos.kun.nl. Name: anonymous.

(22) XMol, version 1.3.1; Minnesota Supercomputing Center, Inc.: Minneapolis, MN, 1993.

(23) Knözinger, H.; Ratnasamy, P. *Catal. Rev. Sci. Eng*. **1978**, *17*, 31.

(24) 1 cal = 4.184 J.

(25) (a) Holm, V. C. F.; Blue, R. W. *Ind. Eng. Chem*. **1951**, *43*, 501. (b) Carleton, F. B.; Gilmore, T. A.; Laverty, T. D.; Rooney, J. J. *J. Chem. Soc. Chem. Commun*. **1977**, 896. (c) Narbershuber, T. F.; Vinnek, H.; Lercher, J. A. *J. Catal*. **1995**, *157*, 388. (d) Narbershuber, T. F.; Brait, T.; Seshan, K.; Lercher, J. A. *J. Catal*. **1997**, *172*, 127.

(26) Frash, M. V.; van Santen, R. A. *J. Phys. Chem. A* **2000**, *104*, 2468.

(27) Narbershuber, T. F.; Stockenhuber, M.; Brait, T.; Seshan, K.; Lercher, J. A. *J. Catal*. **1996**, *160*, 183.

(28) Kazansky, V. B.; Borovkov, V. Yu.; Zaitsev, A. V. *Proc. 9th Intl. Congr. Catal., Calgary* **1988**, *3*, 1426.

(29) Long, M. A.; Garnett, J. L.; Williams, P. G. *Aust. J. Chem*. **1982**, *35*, 1057.

(30) (a) Schoofs, B.; Schuermans, J.; Schoonheydt, R. A. *Micropor. Mesopor. Mater*. **2000**, *35*−*36*, 99. (b) Paravano, C.; Hammel, E. F.; Taylor, H. S. *J. Am. Chem. Soc*. **1948**, *70*, 2269. (c) Hansford, R. C.; Waldo, P. G.; Drake, I. C.; Honig, R. E. *Ind. Eng. Chem*. **1952**, *44*, 1108. (d) Hindin, S. G.; Mills, G. A.; Oblad, A. G. *J. Am. Chem. Soc*. **1955**, *77*, 538. (e) Burwell, R. L., Jr.; Porte, H. A.; Hamilton, W. H. *J. Am. Chem. Soc*. **1959**, *81*, 828. (f) Lapszewicz; J. A.; Jiang, X.-Z. *Catal. Lett*. **1992**, *13*, 103. (g) Iglesia, E.; Baumgartner, J. E. *Catal. Lett*. **1993**, *21*, 545. (h) Sommer, J.; Hachoumy, M.; Garin, F.; Barthomeuf, D. *J. Am. Chem. Soc*. **1994**, *116*, 5491.

(31) (a) Bloch, H. S.; Pines, H.; Schmerling, L. *J. Am. Chem. Soc*. **1946**, *68*, 153. (b) Nenitzescu, C. D.; Avram, M.; Sliam, E. *Bull. Soc. Chem. France* **1955**, 1266. (c) See also: Nenitzescu, C. D.; Cantuniari, I. P. *Ber. Dtsch. Chem. Ges.* **1933**, *66*, 1097.

(32) (a) J. M.Oelderik cited in: Brouwer, D. M.; Mackor, E. L. *Proc. Chem. Soc*. **1964**, 147. (b) Oelderik, J. M.; Mackor, E. L.; Platteeuw, J. C.; van der Wie, A. British Patent 981,311 (appl. 1962), equivalent to U.S. Patent 3,201,494, 1965. (c) Brouwer, D. M.; Hogeveen, H. *Prog. Phys. Org. Chem*. **1972**, *9*, 179.

(33) Fărcaşiu, D.; Siskin, M.; Rhodes, R. P. *J. Am. Chem. Soc*. **1979**, *101*, 7671.

(34) (a) Jacobs, P. A. *Carboniogenic Activity of Zeolites*; Elsevier: Amsterdam, 1977. (b) Mirodatos, C.; Barthomeuf, D. *J. Chem. Soc. Chem. Commun*. **1981**, 39. (c) Jacobs, P. A. *Catal. Rev.-Sci. Eng*. **1982**, *24*, 415. (d) Mihindou-Koumba, P. C.; Lemberton, J. L.; Perot, G.; Guisnet, M. *Nouv. J. Chim*. **1984**, *8*, 31. (e) Patrilyak, K. I.; Bortyshevskii, V. A.; Tsuprik, I. N.; Gutyrya, V. S.; Baiburskii, V. L. *Doklady Akademii Nauk S. S. S. R.* **1985**, *283*, 384. (f) Martens, J. A.; Jacobs, P. A. In ref 2, p 52.

(35) Treatments of alkene hydrogenation/alkane dehydrogenation: (a) Senger, S.; Radom., L. *J. Am. Chem. Soc*. **2000**, *122*, 2613. (b) Kazansky, V. B.; Frash, M. V.; van Santen, R. A. *Catal. Lett*. **1994**, *28*, 211.

(36) (a) Fărcaşiu, D.; Marino, G. M.; Kastrup, R. V.; Rose, K. D. presented at the 185th American Chemical Society National Meeting, Seattle, WA, March 1983, Abstract ORGN 160. (b) Fărcaşiu, D.; Ghenciu, A.; Marino, G.; Rose, K. D. *J. Am. Chem. Soc.* **1997**, *119*, 11826.

(37) (a) Fărcaşiu, D. *J. Chem. Soc. Chem. Commun*. **1994**, 1801. (b) Xu, T.; Munson, E. J.; Haw, J. F. *J. Am. Chem. Soc.* **1994**, *116*, 1962.

(38) (a) Fărcaşiu, D. Lukinskas, P. *J. Chem. Soc., Perkin Trans. 2* **1999**, 1609. (b) Fărcaşiu, D. Lukinskas, P. *J. Chem. Soc., Perkin Trans. 2* **1999**, 2715. (c) Fărcaşiu, D. Lukinskas, P. *J. Chem. Soc., Perkin Trans. 2* **2000**, 2295.

(39) Olah, G. A.; Surya Prakash, G. K. S.; Sommer, J. *Superacids*; Wiley: New York, 1985; p 249.

(40) Sokolovskii, V. D.; Mamedov, E. A. *Catal. Today* **1992**, *14*, 331 (Part 4).

(41) Capitán, M. J.; Odriozola, J. A.; Márquez, A.; Sanz, J. F. *J. Catal*. **1995**, *156*, 273.

(42) (a) Stamires, D. N.; Turkevich, J. *J. Am. Chem. Soc*. **1964**, *86*, 749. (b) Shih, S. *J. Catal*. **1983**, *79*, 390. (c) McVicker, G. B.; Kramer, G. M.; Ziemiak, J. J. *J. Catal*. **1983**, *83*, 286. (d) Fărcaşiu, D.; Ghenciu, A. *Prepr. Div. Pet. Chem., Am. Chem. Soc.* **1994**, *39*, 479. (e) Fărcaşiu, D.; Ghenciu, A.; Li, J. Q. *J. Catal*. **1996**, *158*, 116.

(43) Alvarez, L. J.; Blumenfeld, A. L.; Fripiat, J. J. *J. Chem. Phys*. **1998**, *108*, 1724.

(44) Fărcaşiu, D.; Lee, K.-H. *J. Mol. Catal., A* **2000**, *161*, 213.

(45) Fărcaşiu, D.; Lee, K.-H. *Catal. Commun.* **2001**, *2*, 5.